Supporting information

for

Ammonia Decomposition over Low-loading Ruthenium Catalyst Achieved through "Adiabatic" Plasma Reactor

Minhazur Rahman Shawon,[1] Chinwendu Umeojiakor,[1] Anthony Griffin,[2] Jeffrey Aguinaga,[2] Jiachun Wu,[1] Derek Patton,[2] Zhe Qiang,[2] Hossein Toghiani,[1] Yizhi Xiang[1,3,*]

[1]Dave C. Swalm School of Chemical Engineering, Mississippi State University, Mississippi State, Mississippi 39762, USA

[2]School of Polymer Science and Engineering, The University of Southern Mississippi, Hattiesburg, Mississippi 39406, USA

[3]Department of Chemical and Biomedical Engineering, University of Missouri, Columbia, Missouri 65211, USA

*Corresponding Author, yxpxb@missouri.edu

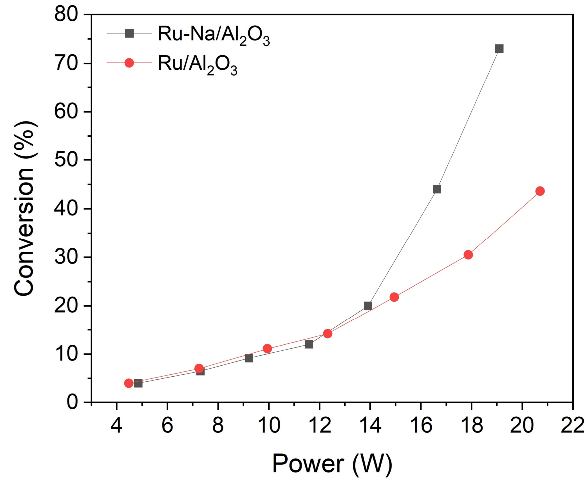

Figure S1. Catalytic performance of NH_3 decomposition in adiabatic plasma reactor over the $Ru_{0.5}/Al_2O_3$ and $Ru_{0.5}$-Na/Al_2O_3 catalysts.

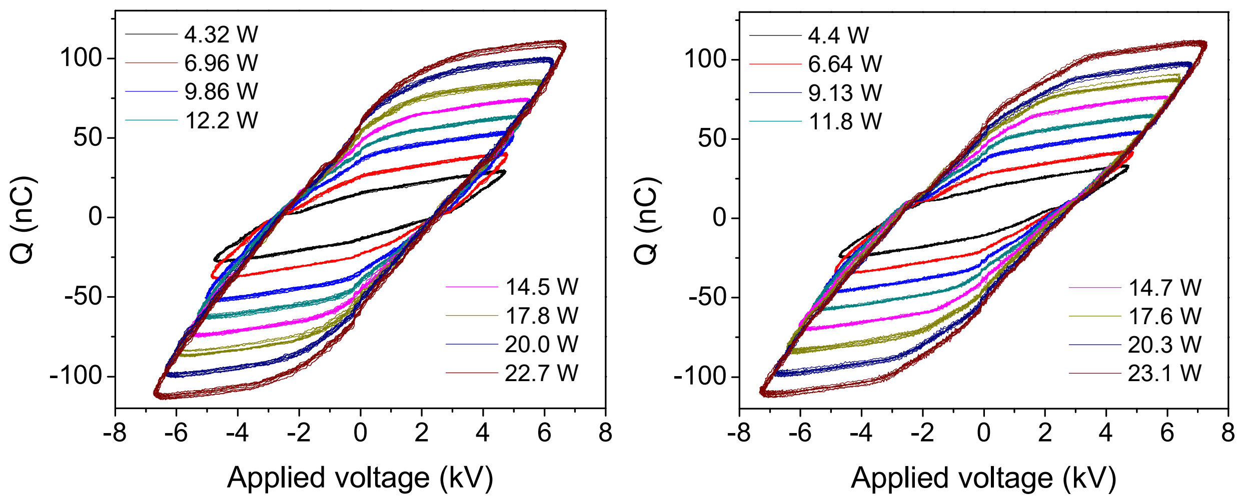

Figure S2. Q-V Lissajours curves of NH_3 discharge at different powers between 4-23 W in adiabatic (left) and nonadiabatic (right) plasma reactor (with a catalyst).

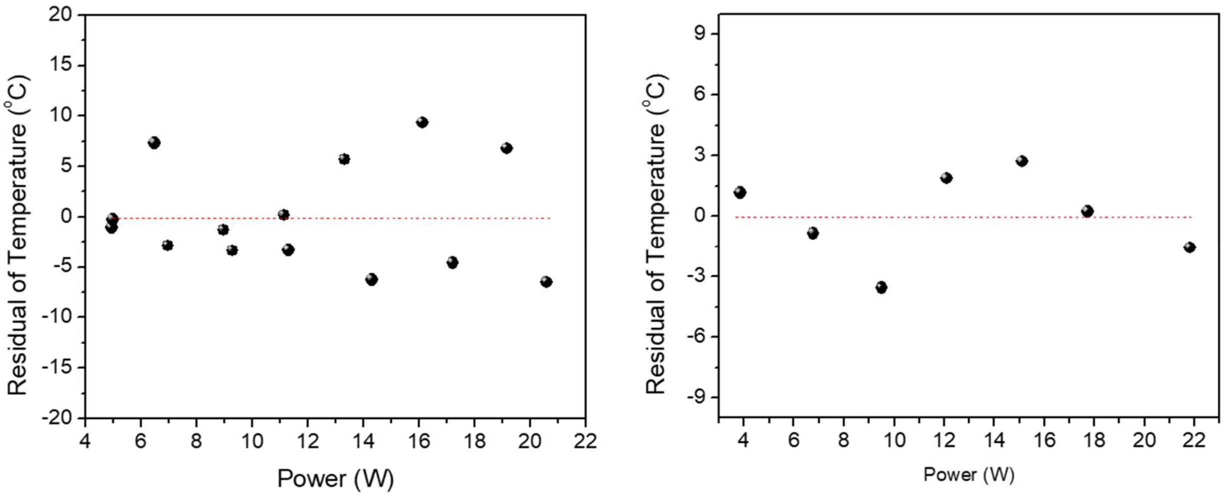

Figure S3. The standard deviation of temperature at different powers from the fitted exponential equation for both adiabatic (left) and nonadiabatic plasma reactors.

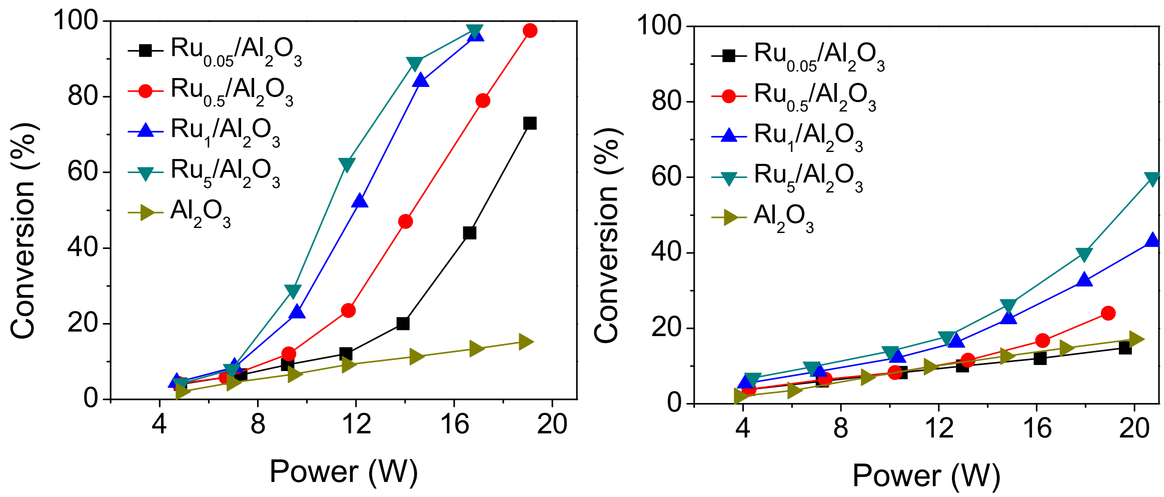

Figure S4. Influence of Ru loading on NH_3 conversion achieved in adiabatic (Left panel) and nonadiabatic (right panel) plasma reactors. The reaction was carried out with 20 mL/min of undiluted NH_3 and 0.1 g of catalyst.

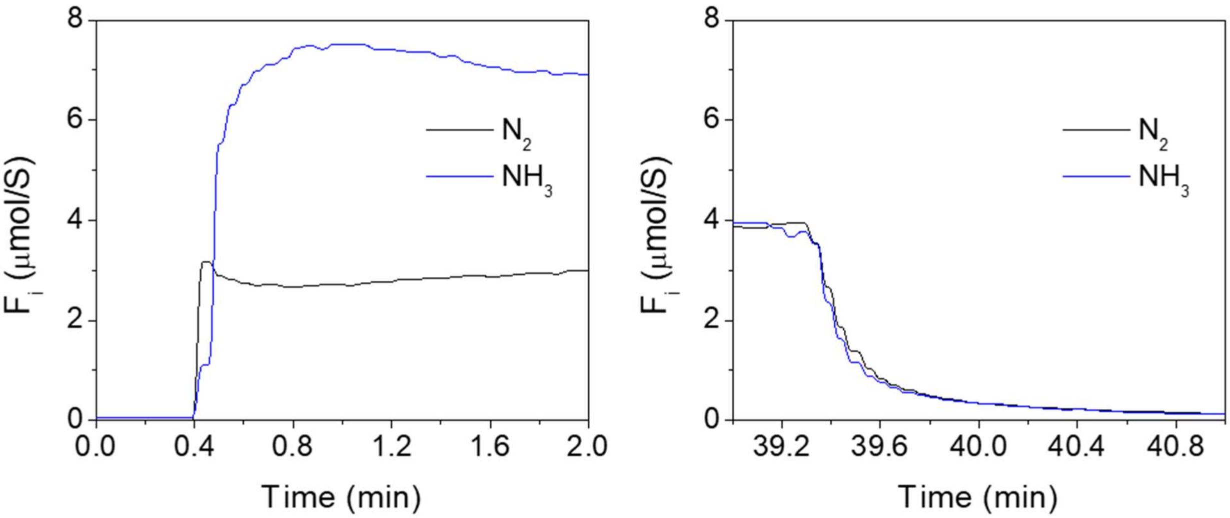

Figure S5. Response of N_2 and NH_3 outlet flow to step changes from Ar to NH_3 and back to Ar with plasma ON. The experiment was carried out with 20 mL/min of undiluted NH_3, 0.1 g of $Ru_{0.5}/Al_2O_3$ catalyst, and plasma power of around 14 W.

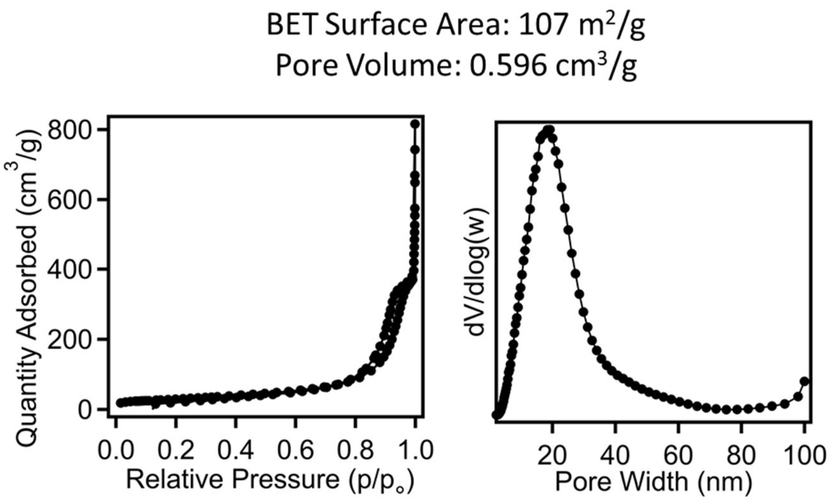

Figure S6. N_2 adsorption/desorption isotherm and pore size distribution of the $Ru_{0.05}/Al_2O_3$ after plasma catalytic NH_3 decomposition.

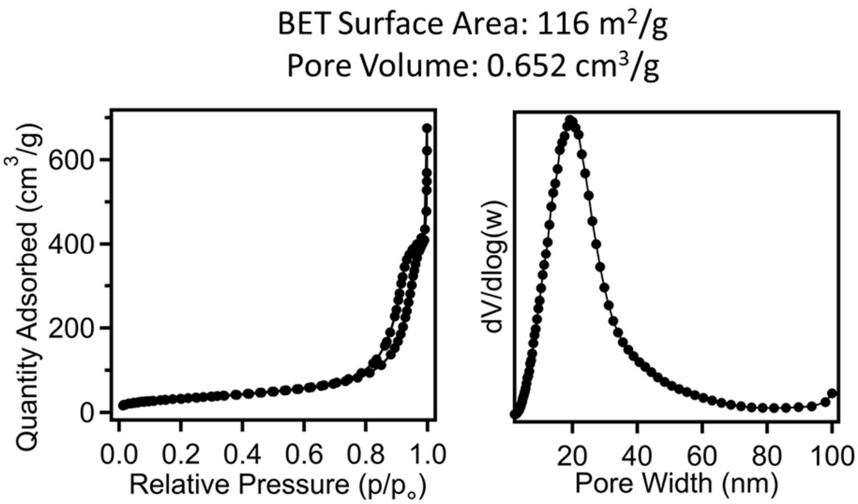

Figure S7. N_2 adsorption/desorption isotherm and pore size distribution of the $Ru_{0.5}/Al_2O_3$ after plasma catalytic NH_3 decomposition.

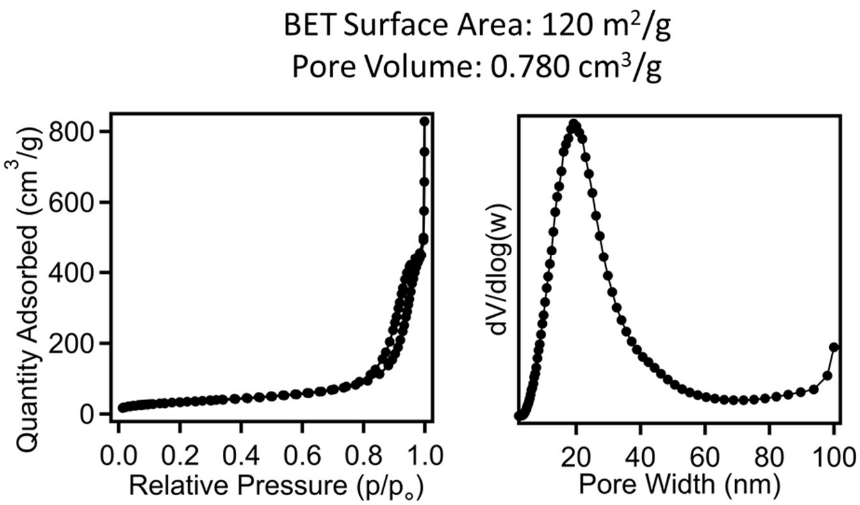

Figure S8. N_2 adsorption/desorption isotherm and pore size distribution of the Ru_1/Al_2O_3 after plasma catalytic NH_3 decomposition.

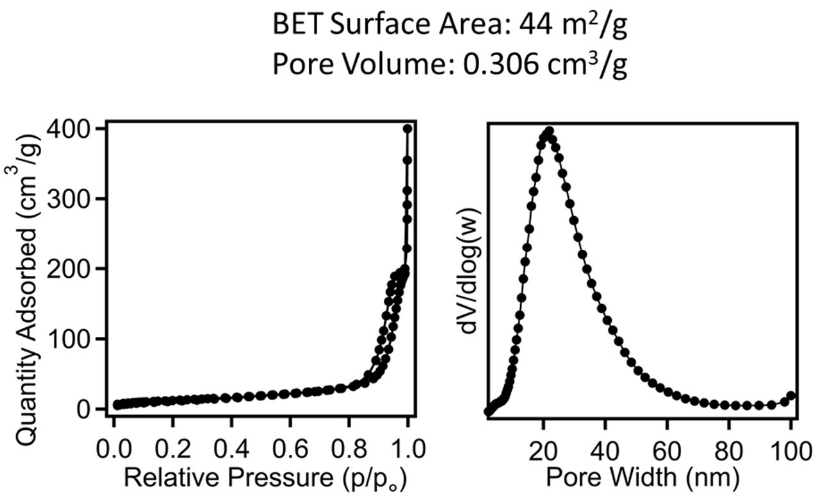

Figure S9. N_2 adsorption/desorption isotherm and pore size distribution of the Ru_5/Al_2O_3 after plasma catalytic NH_3 decomposition.

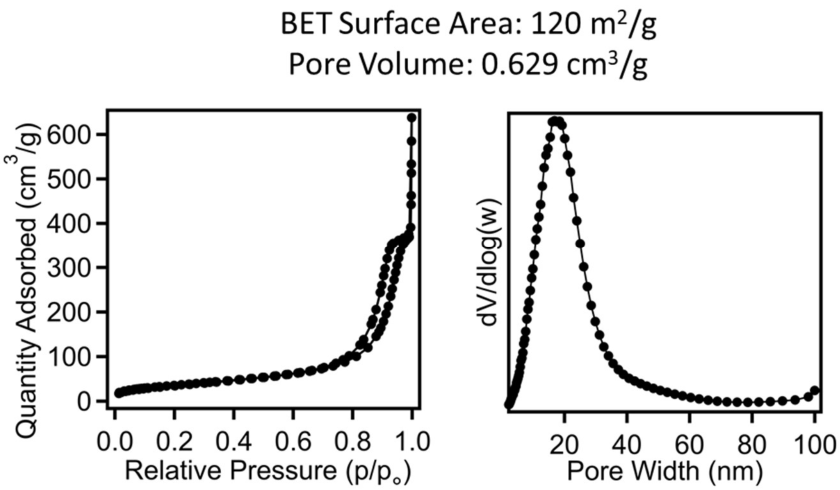

Figure S10. N_2 adsorption/desorption isotherm and pore size distribution of the $Ru_{0.5}/Al_2O_3$ after thermocatalytic NH_3 decomposition.

Table S1. Comparison of catalytic performance of plasma catalytic NH_3 decomposition with the state-of-the-art catalysts.

Catalyst	Power (W)	Temperature (℃)	GHSV ($ml_{NH3}/(g_{cat} \cdot h)$)	Conversion (%)	Reference
0.5 % Ru/Al_2O_3	19	475	12000	99	This work
1 % Ru/Al_2O_3	17	425	12000	99	This work
1.5% Ru/La_2O_3	16	300	2400	65	1
1.5% Ru/La_2O_3	20	375	2400	99	1
Mo_2N	26.4	450	3000	99	2
Co/fumed SiO_2	30	450	2727	99	3
6Fe-4Ni	41	460	14400	61	4
6Fe-4Ni	41	500	14400	99	4

Reference

1. Z. Wang, G. He, H. Zhang, C. Liao, C. Yang, F. Zhao, G. Lei, G. Zheng, X. Mao and K. Zhang, *ChemSusChem*, 2023, **16**, e202202370.
2. Z. Wang, H. Zhang, Z. Ye, G. He, C. Liao, J. Deng, G. Lei, G. Zheng, K. Zhang, F. Gou and X. Mao, *Int. J. Hydrogen Energy*, 2024, **49**, 1375-1385.
3. L. Wang, Y. Yi, Y. Zhao, R. Zhang, J. Zhang and H. Guo, *ACS Catal.*, 2015, **5**, 4167-4174.
4. Y. Yi, L. Wang, Y. Guo, S. Sun and H. Guo, *AIChE J.*, 2019, **65**, 691-701.